

## 1 Title

2 Genomic epidemiology of syphilis reveals independent emergence of macrolide resistance  
3 across multiple circulating lineages

4

## 5 Authors, Affiliations

6 Mathew A. Beale<sup>1</sup>, Michael Marks<sup>2,3</sup>, Sharon K. Sahi<sup>4</sup>, Lauren C. Tantaló<sup>4</sup>, Achyuta V. Nori<sup>5</sup>,  
7 Patrick French<sup>6</sup>, Sheila A. Lukehart<sup>7</sup>, Christina M. Marra<sup>4</sup>, Nicholas R. Thomson<sup>1,8</sup>

8 Corresponding authors: MAB, [mathew.beale@sanger.ac.uk](mailto:mathew.beale@sanger.ac.uk); NRT, [nrt@sanger.ac.uk](mailto:nrt@sanger.ac.uk)

9

10 <sup>1</sup> Parasites and Microbes, Wellcome Sanger Institute, Wellcome Genome Campus, Hinxton,  
11 Cambridgeshire, UK

12 <sup>2</sup> Clinical Research Department, Faculty of Infectious and Tropical Diseases, London School  
13 of Hygiene & Tropical Medicine, London, UK

14 <sup>3</sup> Hospital for Tropical Diseases, London, UK

15 <sup>4</sup> Department of Neurology, University of Washington, USA

16 <sup>5</sup> Guy's & St Thomas' NHS Foundation Trust, London, UK

17 <sup>6</sup> The Mortimer Market Centre CNWL, Camden Provider Services, London, UK

18 <sup>7</sup> Departments of Medicine and Global Health, University of Washington, USA

19 <sup>8</sup> Department of Pathogen Molecular Biology, Faculty of Infectious and Tropical Diseases,  
20 London School of Hygiene & Tropical Medicine, London, UK

21

## 22 Abstract

23 Syphilis is an ancient sexually transmitted infection caused by the bacterium *Treponema*  
24 *pallidum* subspecies *pallidum* and may lead to severe clinical complications. Recent years  
25 have seen striking increases in syphilis diagnoses in many high income countries, with the  
26 UK reporting a 148% increase in new diagnoses over 10 years. The reasons for this rise are  
27 complex and multifactorial, including changing cultural, behavioural, and technological  
28 factors that influence sexual networks and transmission dynamics. Previous genomic  
29 analyses have suggested that one lineage of syphilis, called SS14, may have expanded  
30 recently, with most syphilis caused by this lineage, and that this expansion indicates  
31 emergence of a single pandemic azithromycin-resistant cluster. In this study, we used high  
32 throughput sequencing of *Treponema pallidum* performed on DNA extracted directly from  
33 clinical swab samples and clinically derived samples with minimal passage in the rabbit to  
34 more than double the number of publicly available whole genome sequences. We used  
35 phylogenomic and population genomic analyses to show that both SS14-lineage and  
36 Nichols-lineage *T. pallidum* are present in contemporary patients and that SS14 is a  
37 polyphyletic lineage. We further correlate the appearance of genotypic macrolide resistance  
38 with multiple SS14 sub-lineages, showing that both genotypically macrolide resistant and  
39 macrolide sensitive sub-lineages are spreading contemporaneously. These findings  
40 demonstrate that macrolide resistance has independently evolved multiple times in *T.*  
41 *pallidum*, that once evolved it becomes fixed in the genome and is transmissible, and that

42 these findings are not consistent with the hypothesis of SS14-lineage expansion purely due  
43 to macrolide resistance. Beyond relevance to our understanding of the current syphilis  
44 epidemic, these findings show how macrolide resistance evolves in *Treponema* subspecies.  
45 Furthermore, the evolution of macrolide resistance, despite not being first-line treatment,  
46 provides a warning on broader issues of antimicrobial resistance, and highlights the  
47 importance of stewardship and strategic planning to prevent the emergence of  
48 antimicrobial resistance.

## 49 Introduction

50 Syphilis is an ancient, predominantly sexually transmitted infection (STI) caused by the  
51 bacterium *Treponema pallidum* subspecies *pallidum* (TPA). If untreated, syphilis causes a  
52 multi-system disease that can progress to severe cardiovascular and neurological  
53 involvement, which can be potentially fatal. Syphilis caused a pandemic wave that swept  
54 across Renaissance Europe over 500 years ago, and remained a problem until the  
55 introduction of antibiotics in the post-World War II era<sup>1</sup>. Despite effective treatment with  
56 benzathine benzylpenicillin G (BPG), syphilis transmission levels fluctuated but persisted  
57 throughout the 20<sup>th</sup> century, until the AIDS crisis of the 1980s and 1990s, where changes in  
58 sexual behaviour (and possibly AIDS-related mortality), led to an overall decline in incidence  
59 in many western countries and populations<sup>2,3</sup>.

60

61 Recent years have seen a sharp increase in syphilis cases in many high-income countries,  
62 predominantly within sexual networks of men who have sex with men (MSM)<sup>4,5</sup>. In the  
63 United Kingdom there was a 20% increase in reported new diagnoses between 2016 and

64 2017, and a 148% increase since 2008<sup>6</sup>. Similar trends have been reported in other  
65 countries<sup>4,7</sup>. The reasons for this increase are complex and multifactorial, incorporating  
66 changing behavioural patterns mediated by cultural, societal and technological changes in  
67 our modern world<sup>8</sup>, resulting in a perfect epidemiological storm. It is also possible that there  
68 are bacterial changes either driving the current rise in syphilis incidence, or occurring as a  
69 consequence of this increase. However, current knowledge of TPA is limited, largely because  
70 the bacterium was, until recently, intransigent to *in vitro* culture<sup>9</sup>. Most current  
71 understanding of TPA biology therefore comes from related species or from TPA cultured in  
72 the *in vivo* rabbit testicular model<sup>10</sup>. Genomic analysis has also been limited due to low  
73 levels of TPA pathogen load in patients and difficulty in readily isolating new strains.  
74 Sequencing must be performed directly on clinical specimens or after passage through  
75 rabbits, leading to substantial bottlenecks in genomic data generation. Recent advances  
76 have enabled target enrichment of pathogen reads directly from clinical or cultured  
77 specimens<sup>11,12</sup>, and this was recently employed separately by different groups, including our  
78 own, to sequence TPA and other *T. pallidum* subspecies directly from patient samples<sup>13-15</sup>.

79

80 The availability of increasing numbers of genomic sequences enabled the first description of  
81 the global TPA population structure using 31 near genome-length TPA sequences, along  
82 with a small number derived from closely related species<sup>14</sup>. The authors described two  
83 lineages within TPA; a Nichols-lineage found almost exclusively in North American  
84 sequences exhibiting substantial nucleotide diversity, and a geographically widespread but  
85 genetically homogeneous SS14-lineage, confirming previous analyses using multi-locus  
86 sequence typing<sup>16</sup>. Of these two lineages, they found that 68% of tested TPA genomes

87 belonged to the SS14-lineage, and further analysis using a larger dataset of 1354 single-  
88 locus molecular types (comprising 623 samples from South East Asia, 241 from the USA, 392  
89 from Europe and a small number of other locations) also supported this view (94%  
90 SS14-lineage).

91

92 Although penicillin resistance has never been reported in syphilis, increasing levels of  
93 genotypic resistance, and clinical treatment failure, to macrolides such as azithromycin have  
94 been reported<sup>17,18</sup>, conferred by either one of two single nucleotide polymorphisms (SNPs)  
95 in the 23S ribosomal sequence (A2058G and A2059G). Arora *et al* reported that 90% of  
96 sequenced SS14-lineage genomes and 25% of Nichols-lineage genomes contained SNPs  
97 conferring macrolide resistance; furthermore, they suggested that SS14-lineage may  
98 represent a single pandemic azithromycin-resistant cluster<sup>14</sup>.

99

100 In this study, we performed direct whole genome sequencing on 73 TPA samples from the  
101 US and Europe, and combined these data with 49 publicly available genomes. We used  
102 phylogenetic analysis to delineate sub-lineages within the both the SS14- and Nichols-  
103 lineages, showing striking patterns of the emergence and fixation of macrolide resistance  
104 SNPs that indicate independent evolution and proliferation of resistance alleles. These  
105 findings have implications for our understanding of the increasing incidence of syphilis and  
106 on the potential of the WHO Yaws eradication campaign to drive further development of  
107 macrolide resistance in both TPA and in the closely related *Treponema pallidum* subspecies  
108 *pertenue* (TPP)<sup>19,20</sup>.

109

## 110 Results

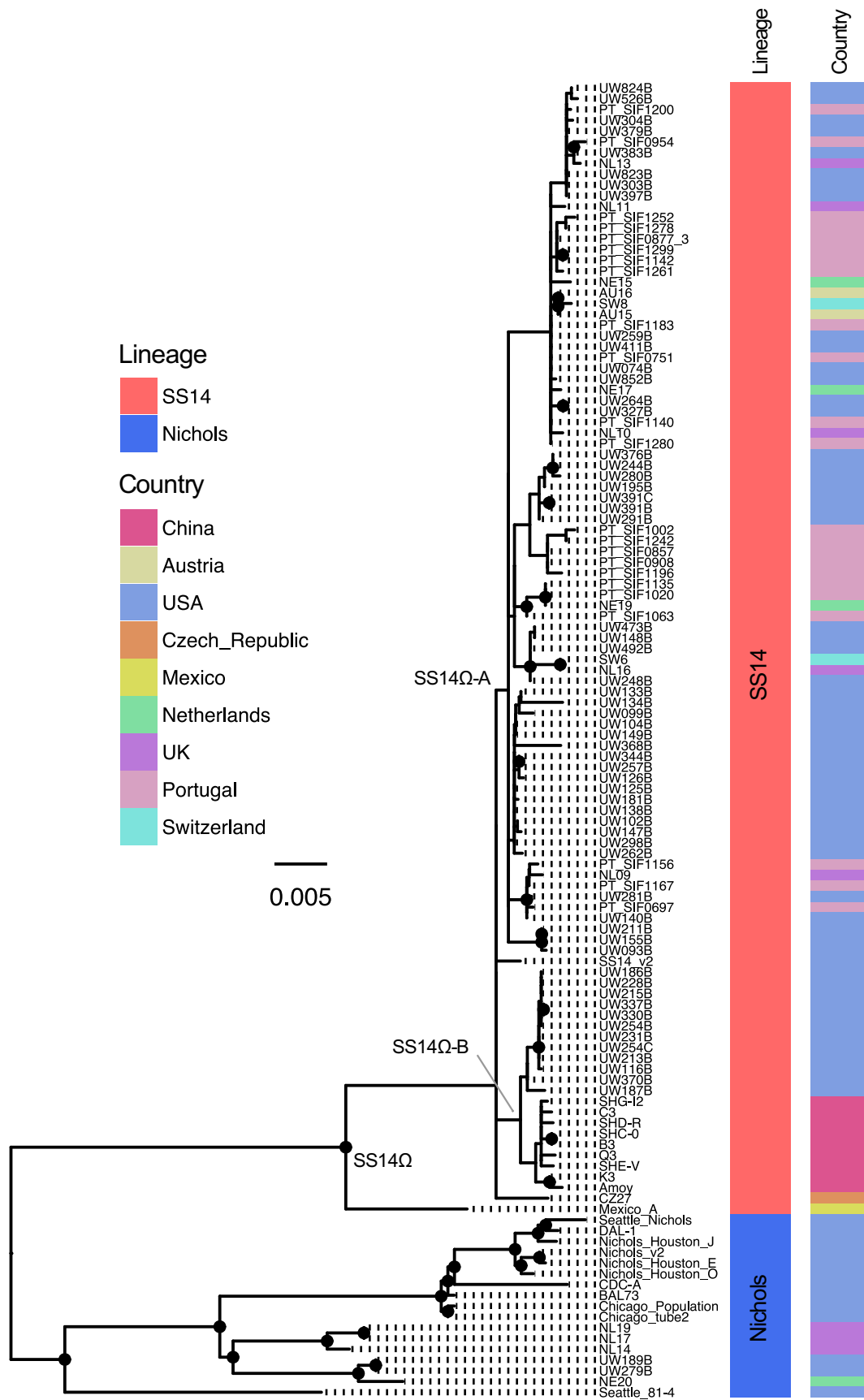
111 We sequenced eight genomes directly from clinical swabs collected in 2016 from patients in  
112 the United Kingdom and 60 isolate genomes from low rabbit passage samples (no more  
113 than two passages from the original patient sample; henceforth referred to as ‘recently  
114 clinically derived’) originally collected from patients between 2001-2011 in the USA. We also  
115 resequenced three clonally derived laboratory strains from the USA that have been  
116 previously sequenced (Nichols Houston E, Nichols Houston J, Nichols Houston O) but remain  
117 unpublished, and two strains for which the sequencing reads were not publicly available  
118 (Chicago<sup>21</sup>, Seattle 81-4<sup>22</sup>). We combined our data with 49 high-quality genomes published  
119 previously<sup>13,14,23–28</sup>, 41 of which were recently derived from clinical patients, yielding a  
120 dataset of 122 genomes (109 with limited passage from clinical patients). Combined, our  
121 sample set included 72 genomes from the USA (predominantly Seattle), 8 from the UK  
122 (exclusively London), 9 from China (predominantly Shanghai), 23 from Portugal (exclusively  
123 Lisbon), and a small number from other countries, all collected between 1912-2016  
124 (Supplementary Table 1).

125

126 After removal of recombinant and repetitive sites (both by selective mapping and screening  
127 – see Methods and Supplementary Table 2), we performed phylogenomic analyses, using  
128 maximum likelihood and Bayesian methods to define lineages. In agreement with previous  
129 studies<sup>14</sup>, we show the presence of two dominant lineages in our dataset (previously  
130 denoted SS14 and Nichols; Figure 1) that are separated by >70 non-recombining single

131 nucleotide polymorphisms (SNPs). Of the 122 total samples included in this study, 105 (86%)  
132 belonged to the SS14-lineage, whilst of the 109 clinical samples included, 103 (94%) were  
133 from SS14-lineage. In contrast, only six Nichols-lineage samples were recently clinically  
134 derived, and most (11/17) Nichols-lineage genomes examined were historically passaged  
135 isolates, including those derived from the original Nichols strain isolated in 1912 and  
136 disseminated to different North American laboratories; some Nichols-lineage genomes  
137 represent clones of the parent strain derived *in vivo*. However, although we observed a  
138 strong bias towards clinically derived SS14-lineage samples in this dataset, not all recent  
139 clinical strains were of the SS14-lineage; six recent clinical samples belonged to the Nichols-  
140 lineage, three (of eight sequenced) clinical samples from the UK in 2016, one collected in  
141 the Netherlands in 2013, and two from the USA in 2004, indicating that transmission of this  
142 lineage is ongoing and potentially more widespread than previously thought.

143





145 Figure 1. Maximum likelihood phylogeny of 122 high quality *T. pallidum* subspecies *pallidum*  
146 genomes (including clinical and non-clinically derived samples), showing lineage and country  
147 of origin. Ultra-Fast bootstrap values  $\geq 95\%$  are labelled with black nodes points. Branches  
148 are scaled by mean nucleotide substitutions/site.

149

150 Bayesian phylogenetic reconstruction was used to date the time to most recent common  
151 ancestor (TMRCA) for the different TPA lineages. However, temporal analysis of heavily  
152 passaged laboratory strains (such as those derived from the original Nichols isolate) is  
153 problematic because the true mutational age may be unknown, meaning coalescent date is  
154 difficult to infer; we therefore removed extensively passaged strains or strains with no  
155 record of their passage history from this particular part of the analysis. This included the  
156 removal of the Nichols and SS14 reference strains, as well as the Mexico A strain that  
157 delineated the SS14 $\Omega$  lineage described previously<sup>14</sup>. Root-to-tip regression analysis of the  
158 remaining 109 clinical genomes indicated that TPA possesses a clock-like signal  
159 (Supplementary Figure 1), and we performed Bayesian phylogenetic reconstruction and tip  
160 date analysis using BEAST<sup>29</sup> under a Strict Constant model, inferring a median molecular  
161 clock rate of  $2.28 \times 10^{-7}$ , or 0.26 sites/genome/year (meaning we would expect TPA genomes  
162 on average to accumulate one SNP every four years by natural drift). We inferred a  
163 temporal timeline for the tree, and our analysis broadly supported previous estimates<sup>14</sup>  
164 dating the separation of Nichols- and SS14 at around the mid 18<sup>th</sup> Century (median date  
165 1755, 95% HPD 1651–1835; Figure 2A).

#### 166 SS14-lineage shows a polyphyletic structure

167 Within the SS14-lineage, the high number of full-length sequences enabled fine-scale  
168 description of phylogenetic sub-structure. In particular, we show partitioning of the SS14 $\Omega$   
169 centroid cluster previously defined<sup>14</sup> into two lineages; one composed of European and  
170 North American derived samples (SS14 $\Omega$ -A), and another of Chinese and North American  
171 derived samples (SS14 $\Omega$ -B) (Figure 1). While the American and European samples belonging  
172 to the former SS14 $\Omega$ -A lineage are geospatially admixed, those of the latter SS14 $\Omega$ -B lineage

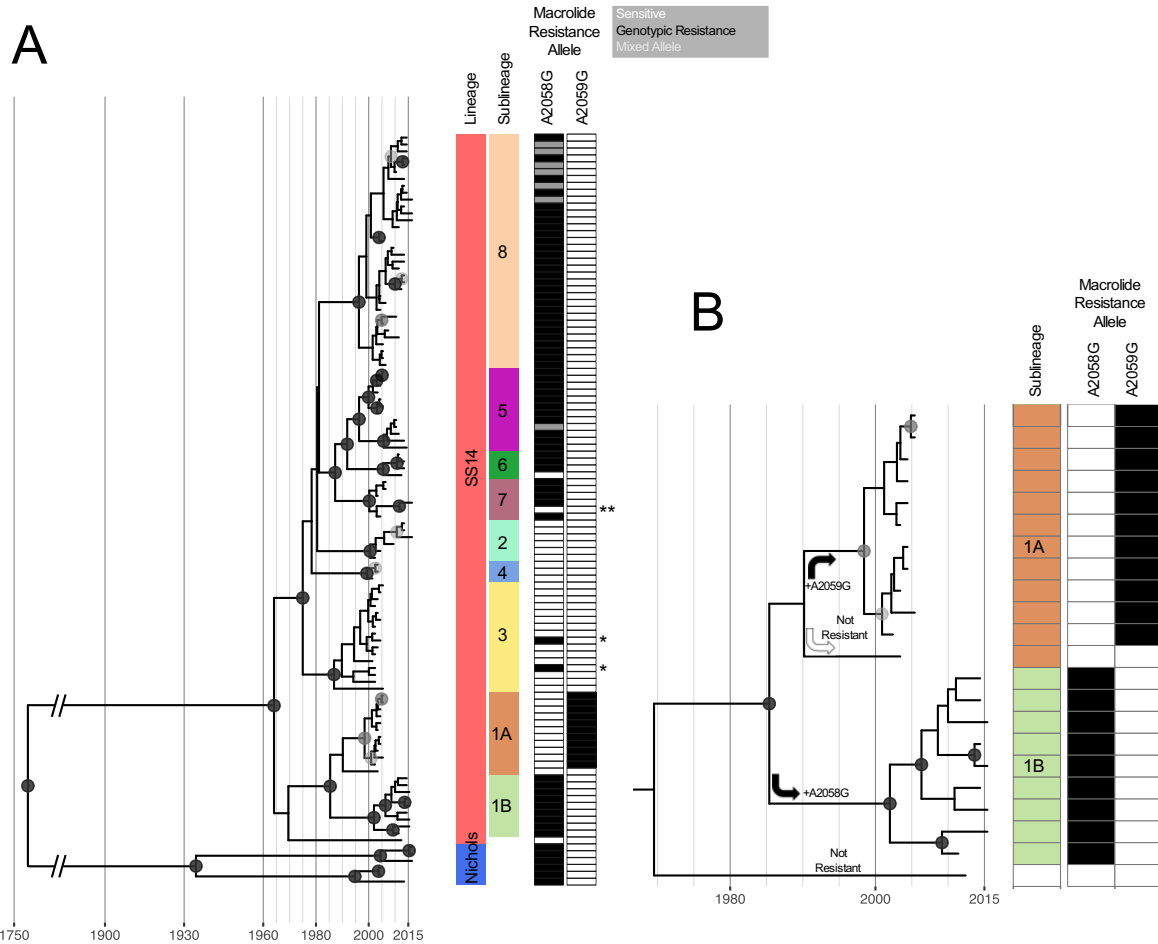
173 can be further separated between Chinese and North American samples. These partitions  
174 were well supported in our maximum likelihood (Figure 1) and Bayesian phylogenies (Figure  
175 2A), as indicated by black node points. We used the rPinecone package<sup>30</sup> to formally classify  
176 these sub-lineages based on a defined root-to-tip SNP distance, identifying eight sub-  
177 lineages (one of which we further subdivided into sublineages 1A and 1B to aid analysis  
178 based temporal and geospatial divergence) within SS14-lineage that correlated well with the  
179 population structure described by the phylogeny (Figure 2A). Importantly, while some nodes  
180 close to the tips in our phylogeny are unsupported due to small numbers of differentiating  
181 SNPs, all sub-lineages defined by rPinecone are supported by >91% posterior support at the  
182 key nodes in our Bayesian phylogeny (Figure 2A).

183

184

185

186



187

188 Figure 2. Bayesian maximum credibility phylogeny of sequences recently derived from  
 189 clinical samples shows expansion of discrete sub-lineages within SS14-lineage, with  
 190 independent evolution of macrolide resistance. A – Time-scaled phylogeny of all clinical  
 191 genomes. Coloured tracks indicate lineage, sub-lineage, and presence of macrolide  
 192 resistance conferring 23S rRNA SNPs (black=present, white=absent, grey=mixed). Node  
 193 points are shaded according to posterior support (black  $\geq 96\%$ , dark grey  $> 91\%$ , light grey  
 194  $> 80\%$ ). \*Sporadic (non-lineage associated) gain of resistance is highlighted in sub-lineage 3  
 195 (samples UW133B and UW262B). \*\*Possible reversion from resistant to wildtype (sample

196 SW6). B – Expanded view of sub-lineages, showing independent acquisition and fixation of  
197 macrolide resistance alleles.

198

199 Macrolide resistance has evolved independently within SS14

200 The molecular basis for macrolide resistance has been well documented in *T. pallidum*, and  
201 is mediated by point mutations in the 23S ribosomal RNA gene at nucleotide positions 2058  
202 and 2059<sup>31-33</sup>. The A2058G variant was first identified in *T. pallidum* Street Strain-14 (the  
203 prototype sample for the SS14-lineage), isolated as long ago as 1977<sup>31</sup>, yet resistance has  
204 not previously been analysed in context with a detailed whole genome phylogeny. We used  
205 ARIBA<sup>34</sup> to perform localised assembly and variant calling of treponema-specific 23S  
206 ribosomal sequences from all genomes, and these data were used to infer the presence of  
207 both A2058G and A2059G 23S variants that confer macrolide resistance<sup>31</sup>. *T. pallidum*  
208 possesses two copies of the 23S ribosomal RNA gene, yet previous analyses have not  
209 identified heterozygosity between these two copies – where resistance alleles have been  
210 sequenced, they are homozygous between 23S copies, and it has been suggested a gene  
211 conversion unification mechanism may exist to facilitate this<sup>18</sup>. Of the 122 genomes, 83  
212 showed evidence of genotypic resistance to macrolides, with 76 genomes showing >95%  
213 read support for either the A2058G or A2059G variant. Since it is not possible to  
214 discriminate between short reads originating from either copy of 23S because they are  
215 perfect repeats, this suggests that both copies carry the same resistance mutation. Seven  
216 clinically derived genomes (one UK sample from this study, six described by Pinto and  
217 colleagues<sup>13</sup>) showed a mixed 23S allelic profile. All of these samples had >179x read  
218 coverage for those sites, with only a fraction of reads (26% - 94%) possessing a resistance  
219 allele. In these cases it was not possible to clearly distinguish between a mixture of  
220 homozygous positive and negative bacteria in the same patient (either due to within-host  
221 evolution or coinfection with multiple strains) or heterozygous sequences from a single  
222 bacteria (different 23S rRNA alleles at each copy; heterozygosity in phase) (Figure 2A).

223

224 Within the 122 genomes included in this study, we observed that 67% (70/105) of SS14-  
225 lineage samples and 35% (6/17) of Nichols-lineage samples were homozygous for either  
226 A2058G or the A2059G 23S rRNA allele. In the SS14-lineage, samples possessed either the  
227 A2058G (n=59) or the A2059G (n=11) variant. In the Nichols-lineage, six possessed a  
228 resistance allele, of which all showed the A2058G variant, and all were from recent clinically  
229 derived samples.

230

231 To explore the emergence of macrolide resistance, we correlated the taxa in our time-scaled  
232 phylogeny with the presence of resistance alleles (Figure 2A). We observed a strong  
233 correlation between our well supported sub-lineages and genotypic macrolide resistance or  
234 sensitivity, such that resistance appears to have evolved on multiple occasions in a stepwise  
235 manner (Figure 2A). For example, Figure 2B shows how the wildtype ancestor of sub-lineage  
236 1B sequences evolved the A2058G between the late 1980s and late 1990s, contrasting with  
237 sub-lineage 1A sequences which did not gain A2058G, but subsequently and independently  
238 evolved the A2059G variant.

239

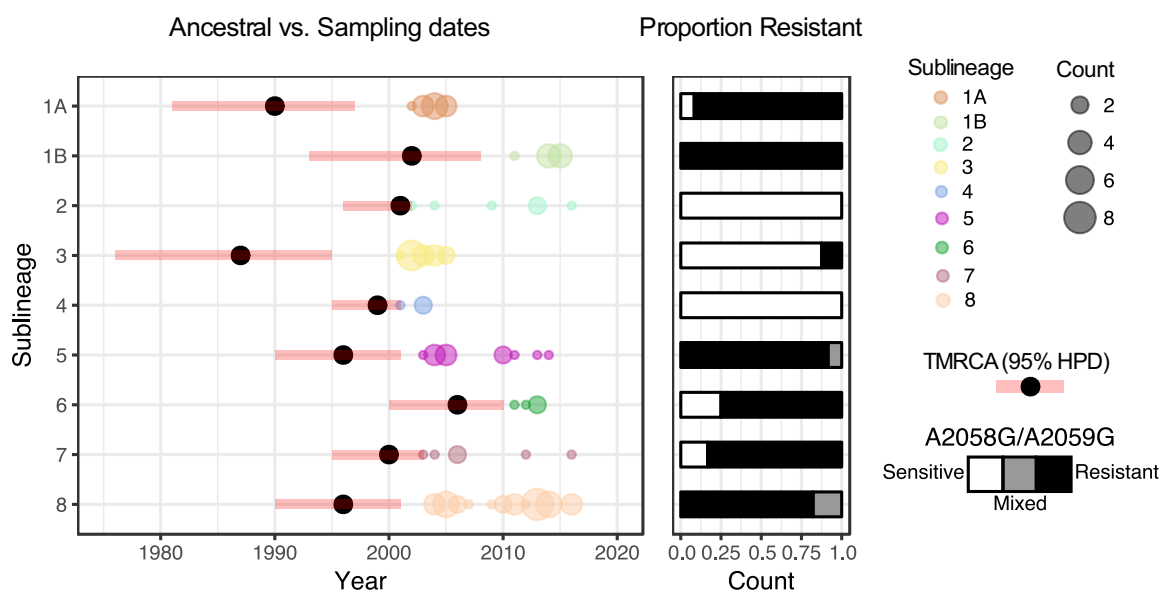
240 More broadly in the phylogeny, we observe that similar independent 23S rRNA mutations  
241 have occurred on at least four occasions (Figure 2A), with separate sub-lineages  
242 characterised by either predominantly macrolide resistant or sensitive genotypes; six of the  
243 nine sub-lineages were predominantly resistant to macrolides, with three sub-lineages  
244 being predominantly sensitive. Several of the macrolide sensitive sub-lineages (in particular

245 sub-lineage 3) contained similar numbers of samples as many of the resistant sub-lineages  
246 (Figure 3), suggesting ongoing selection for macrolide resistance has not influenced the  
247 expansion of these sub-lineages.

248

249 To examine sub-lineage expansion in greater detail, we extracted sampling dates according  
250 to sub-lineage, and correlated these data with the predicted time to most recent common  
251 ancestor (TMRCA) (Figure 3). Whilst all clinical sequences included in this analysis were  
252 sampled after 2000, our analysis indicates that the origins of most of the sub-lineages  
253 predated this time and likely arose during the 1990s (Figure 3). Regarding whole sub-lineage  
254 associated resistance, we also observed more recent sporadic appearance of resistance  
255 mutations, with two separate A2058G variants detected in sub-lineage 3 (an otherwise  
256 macrolide sensitive sub-lineage)(Fig. 2).

257



258



259 Figure 3. Macrolide resistant and sensitive SS14 sub-lineages evolved independently prior to  
260 2006 and expanded equally regardless of resistance genotype. Figure 3 shows sample  
261 collection dates grouped by sub-lineage, with size of circle proportional to number of  
262 sequences, and showing predicted time to most recent common ancestor (TMRCA) with  
263 95% highest posterior density (HPD), and proportion of genotypically macrolide resistant,  
264 sensitive and mixed samples.

## 265 Discussion

266 Compiling the largest *Treponema pallidum* subspecies *pallidum* sequence collection to date,  
267 we show that the majority of the contemporary samples sequenced here were from the  
268 SS14-lineage, consistent with other reports<sup>14</sup>. However, three of eight UK genomes (38%)  
269 belonged to the Nichols-lineage, showing that these two lineages are still circulating  
270 concurrently, and that the prevalence of Nichols-lineage strains may vary by sampling  
271 population.

272

273 We were able to reconstruct a time-scaled phylogeny using only recently clinically derived  
274 samples, and the increase in whole genome sequence numbers combined with the removal  
275 of heavily passaged samples contrasts with previous approaches<sup>14,23</sup>. Arora *et al.* reported a  
276 mean evolutionary rate of  $6.6 \times 10^{-7}$  substitutions/site/year for *T. pallidum*<sup>14</sup>, comparable  
277 with free-living bacterial pathogens with environmental life cycles such as *Vibrio cholerae*  
278 ( $6.1 \times 10^{-7}$ )<sup>35</sup> and *Shigella sonnei* ( $6.0 \times 10^{-7}$ ). However, *T. pallidum* is a host-restricted  
279 pathogen with substantial periods of latency, and as such we would expect a molecular  
280 clock rate more similar to that of *Chlamydia trachomatis* ( $2.15 \times 10^{-7}$ )<sup>36</sup>. Our inferred rate for  
281 TPA ( $2.28 \times 10^{-7}$ ) is consistent with this expectation, as well as with other observations that  
282 suggest *T. pallidum* has a low evolutionary rate<sup>37</sup>.

283

284 Within the SS14-lineage, we defined nine well supported sub-lineages that all diverged from  
285 their most recent common ancestors prior to 2006, with the earliest (sub-lineage 3)  
286 potentially emerging at the end of the 1980s. We observed clear associations between

287 these nine sub-lineages and the presence of macrolide resistance conferring SNPs, with  
288 each sub-lineage dominated by either macrolide resistant (n=6) or macrolide sensitive (n=3)  
289 samples; there were no sub-lineages representing an even mix of resistance genotypes.  
290 Such observations are not consistent with the hypothesis of an ancestrally resistant SS14-  
291 lineage driven to high frequency in the population due to a fitness advantage conferred by  
292 macrolide resistance, where we would expect to see expansion of a single resistant lineage.  
293 Rather, we see evidence of multiple sub-lineages independently evolving macrolide  
294 resistance alleles, as a likely consequence of intermittent selective pressure from macrolide  
295 treatment, consistent with molecular typing data from Seattle<sup>38</sup>. Phylogenetic  
296 reconstruction shows *de novo* evolution of macrolide resistance in syphilis is not a rare  
297 event, and furthermore, when resistance evolves in a lineage, it persists in descendants,  
298 resulting in transmission from person to person. That the variants appear stable within  
299 lineages, with only a single instance in the phylogeny that might represent reversion to a  
300 wildtype state, suggests that there is no strong fitness cost associated with possessing these  
301 macrolide resistance mutations.

302

303 Although our data strongly suggest that global expansion of the SS14-lineage is not  
304 contingent on macrolide resistance, the global increases seen in macrolide resistant  
305 syphilis<sup>18</sup>, as well as the number of resistant lineages emerging in our data, are a cause for  
306 concern. Macrolides such as azithromycin are not considered frontline treatment for  
307 syphilis, with WHO and US guidelines recommending treatment with BPG<sup>39,40</sup>, with  
308 doxycycline recommended as a secondary treatment option. In contrast, WHO now  
309 recommends azithromycin rather than BPG as the treatment of choice for mass drug

310 administration and the eradication of yaws<sup>19</sup>, caused by the closely related *T. pallidum*  
311 subspecies *pertenue*. Macrolide resistance has recently been described in yaws<sup>20</sup> and our  
312 data suggest that further independent evolution of azithromycin resistance is highly likely,  
313 which would have significant implications for yaws eradication efforts. Worryingly, applying  
314 azithromycin-based mass drug administration to populations infected with both TPP and  
315 TPA could promote resistance in both species.

316

317 Several factors are likely to have driven the repeated evolution and subsequent expansion  
318 of macrolide resistant lineages of TPA. Use of azithromycin, or other macrolides, for other  
319 indications is likely to have played a significant role<sup>41</sup>. Azithromycin entered global markets  
320 between 1988 and 1991 (marketed by Pfizer as Zithromax), and became one of the most  
321 widely used antibiotics in the United States for a wide variety of indications<sup>42</sup>, including the  
322 treatment of respiratory tract infections and for the treatment of other sexually transmitted  
323 infections. In many cases, the dose used for treatment of these indications is lower than the  
324 recommended dose for the treatment of syphilis. Azithromycin and clarithromycin were  
325 also widely used prophylactically amongst individuals living with HIV prior to the widespread  
326 availability of combined anti-retroviral therapy. Off-target macrolide exposure is of  
327 particular concern because azithromycin has a long half-life<sup>43</sup> and may persist at subclinical  
328 concentrations in patients. Widespread use of macrolides for this broad range of indications  
329 might therefore have contributed to sub-therapeutic exposure of patients with incubating  
330 or early syphilis and ultimately selection of resistance.

331

332 The recent increase in incidence of syphilis in high income countries likely reflects changes  
333 in sexual behaviour<sup>8</sup>. The fact that we observe the expansion of both genotypically resistant  
334 and sensitive lineages highlights particular treatment issues. There have been significant  
335 global shortages of BPG<sup>44</sup> in low, middle, and high income nations, including the United  
336 States, with the global supply of BPG dependent on just three manufacturers of the active  
337 ingredient<sup>44</sup>. Pharmaceutical production of sterile, injectable  $\beta$ -lactam derived  
338 antimicrobials such as BPG is costly, yet as an older off-patent medication with declining  
339 demand in the face of growing antimicrobial resistance (AMR) in other organisms, the  
340 financial rewards for production are low<sup>44</sup>. This may be compounded by a misperception  
341 that BPG is an outdated drug that could be replaced by newer, more effective drugs<sup>44</sup>. In  
342 circumstances where azithromycin is used instead of doxycycline as second line treatment, a  
343 shortage of BPG leads inevitably to inadequate treatment of early infectious syphilis and  
344 contributes to ongoing, unchecked transmission. In China for example, studies have  
345 reported that despite high rates of macrolide resistance,<sup>45</sup> clinicians have inappropriately  
346 been resorting to macrolide treatment due to ongoing BPG shortages<sup>46</sup>. Thus although a  
347 well-established, highly effective treatment for syphilis (BPG) has been available since the  
348 mid-1950s, shortages in the present era contribute to suboptimal treatment strategies and  
349 continued use of drugs with a known resistance problem.

350

351 The epidemic of syphilis and the widespread problems of azithromycin resistance and BPG  
352 shortage require a multi-faceted response. This includes new strategies for treatment and  
353 reduction of transmission, finding ways to improve the security of the BPG supply chain, and  
354 strengthening molecular surveillance for antimicrobial resistance in *T. pallidum*<sup>47</sup>. Many

355 authors have discussed the importance of rethinking the economics of antimicrobial  
356 development pipelines to ensure we are still able to treat infections<sup>48,49</sup>. In syphilis, we must  
357 rethink how we can protect the continued production of existing highly efficacious  
358 penicillins in the face of increasing antimicrobial resistance rendering them ineffective for  
359 other organisms, especially in the light of the recent increases in syphilis incidence in  
360 Europe, North America, and Asia.

361

## 362 [Materials and Methods](#)

### 363 Samples

364 UK samples consisted of residual DNA, extracted from clinical swabs using a QIAasympphony  
365 (Qiagen) from routine diagnostic samples obtained from patients presenting with clinical  
366 evidence of syphilis at the Mortimer Market Centre, London. Use of the UK samples was  
367 approved by the NHS Research Ethics Committee (IRAS Project ID 195816). US samples  
368 from Seattle were collected from individuals enrolled in a study of cerebrospinal fluid  
369 abnormalities in patients with syphilis, with ethical approval at the University of Washington  
370 (UW IRB # STUDY00003216). Specifically, 2.4-3.0 ml participant blood was inoculated into  
371 rabbit testes as previously described<sup>50</sup>, and *T. pallidum* suspensions were collected after the  
372 second round of passage. Historical strains were propagated in rabbits and harvested from  
373 infected testes. *T. pallidum* suspensions were treated using a lysis buffer (10mM Tris pH 8.0,  
374 0.1M EDTA pH 8.0, 0.5% SDS), freeze-thaw, and extraction using QIAamp Mini kit (Qiagen)  
375 according to the manufacturer's instructions; in select cases the proteinase K incubation  
376 was extended overnight to improve DNA yield. Treponemal DNA was quantified using a

377 qPCR targeting the Tp0574 gene that is conserved across all known members of the  
378 *T. pallidum* cluster, and compared to a standard curve derived from a plasmid containing  
379 the PCR amplicon. Samples with a concentration >2000 genome copies/ $\mu$ l were selected for  
380 sequencing; borderline samples with high volume and a pathogen load over 500 genome  
381 copies/ $\mu$ l were concentrated using a vacuum centrifuge. Samples were arranged in groups  
382 of 20 according to similar (within 2  $C_T$ ) treponemal load, with high concentration outlier  
383 samples diluted as necessary. We added 4 $\mu$ l pooled commercial human gDNA (Promega) to  
384 all samples to ensure total gDNA > 1 $\mu$ g/35 $\mu$ l, sufficient for library prep.

### 385 Sequencing

386 Genomic DNA was sheared to 100-400bp by ultrasonication, followed by adaptor ligation  
387 and index barcoding according to existing Illumina protocols. Samples were pooled in the  
388 preassigned groups of 20 to generate equimolar Total DNA pools. Each pool was then  
389 hybridised using SureSelect 120-mer RNA baits designed against published RefSeq examples  
390 of *T. pallidum* and *T. paraluiscauniculi* as described previously<sup>15</sup>. Libraries were subjected to  
391 125bp paired end sequencing on Illumina HiSeq 2500 with version 4 chemistry according to  
392 established protocols. Raw sequencing reads were deposited at the European Nucleotide  
393 Archive (ENA) under project PRJEB20795; all accessions used in this project are listed in  
394 Supplementary Table 1.

### 395 Sequence analysis and phylogenetics

396 Treponemal sequencing reads were prefiltered using a Kraken<sup>51</sup> v0.10.6 database containing  
397 all bacterial and archaeal nucleotide sequences in RefSeq, plus mouse and human, to  
398 identify and extract those reads with homology to Treponema species, followed by adaptor  
399 trimming using Trimmomatic<sup>52</sup> v0.33. To reduce bias due to variable read depth, as well as

400 make analysis computationally tractable, for samples with high read counts we used seqtk  
401 v1.0 (available at <https://github.com/lh3/seqtk>) to randomly down-sample the binned and  
402 trimmed reads to 2,500,000 unique treponemal read pairs. For publicly available genomes,  
403 raw sequencing reads were downloaded from SRA and subjected to the same binning and  
404 down-sampling pipeline. For a small minority of public genomes, raw sequencing reads were  
405 not available; for these we simulated 125bp PE perfect reads from the RefSeq closed  
406 genomes using Fastaq (available at <https://github.com/sanger-pathogens/Fastaq>).

407

408 For phylogenetic analysis, we used a reference mapping approach with a custom version of  
409 the SS14 v2 reference sequence (NC\_021508.1) from which we first masked 14 highly  
410 repetitive or recombinogenic genes (12 repetitive Tpr genes A-L, arp and TPANIC\_0470)  
411 using bedtools<sup>53</sup> v2.17.0 'maskfasta'. We mapped prefiltered sequencing reads to the  
412 reference using BWA mem<sup>54</sup> v0.7.17 (MapQ  $\geq$  20), followed by indel realignment using  
413 GATK<sup>55</sup> v3.4-46 IndelRealigner, deduplication with Picard MarkDuplicates v1.127 (available  
414 at <http://broadinstitute.github.io/picard/>), and variant calling and consensus  
415 pseudosequence generation using samtools v1.2<sup>56</sup> and bcftools v1.2, requiring a  
416 minimum of three supporting reads per strand and eight in total to call a variant, and a  
417 variant frequency/mapping quality cut-off of 0.8; sites not meeting these criteria were  
418 masked to 'N' in the pseudosequence. Importantly, reads mapping to multiple genomic  
419 positions were marked and excluded from SNP calling, meaning repeated regions such as  
420 the duplicated 23S genes was not included in the multiple sequence alignment used to  
421 derive the phylogenies.

422



423 Multiple sequence alignments were screened for evidence of recombination using  
424 Gubbins<sup>57</sup>, generating recombination-masked full genome length and SNP-only alignments.  
425 Maximum likelihood phylogenies were calculated on SNP-only alignments using IQ-Tree  
426 v1.6.3<sup>58</sup>, correcting for missing constant sites using the built in ascertainment bias  
427 correction<sup>59</sup>, allowing the built-in model testing<sup>60</sup> to determine a K3P (three substitution  
428 types model and equal base frequencies) substitution model<sup>61</sup> with a FreeRate model of  
429 heterogeneity<sup>62</sup> assuming three categories, and performing 1000 UltraFast Bootstraps<sup>63,64</sup>.

430

431 To determine SS14 sub-lineages, we recalculated a maximum likelihood tree as described  
432 above for SS14-clade sequences only (using the Mexico A strain, NC\_018722.1 as outgroup),  
433 before performing a joint ancestral reconstruction<sup>65</sup> of SNPs on the tree branches using  
434 pyjar (available at <https://github.com/simonrharris/pyjar>). We then used the rPinecone  
435 package<sup>64</sup> (available at <https://github.com/alexwailan/rpinecone>), which applies a root-to-  
436 tip approach to defining clusters based on SNP distance relative to ancestral nodes. We used  
437 a cluster threshold of 10 SNPs, which proved optimal for describing the underlying  
438 phylogenetic structure of the tree, and yielded eight sub-lineages. Within sub-lineage 1, we  
439 found that pinecone clusters did not accurately represent the phylogeny, despite a clear  
440 phylogenetic separation, with one group of sequences from China associated with the  
441 A2058G allele, and the other group from the USA associated with the A2059G allele. We  
442 further manually clustered these sequences according to their shared ancestral nodes,  
443 naming them sublineages 1A and 1B.

444

445 We evaluated our maximum likelihood phylogeny for evidence of temporal signal using  
446 TempEst<sup>66</sup> v1.5, and this showed a correlation of 0.44 and  $R^2$  of 0.20 for the whole tree  
447 (Supplementary Figure 1), whilst the SS14-lineage -only alignment showed a correlation of  
448 0.66 and  $R^2$  of 0.44; this indicated that there was sufficient evidence for temporal signal and  
449 we proceeded to BEAST analysis. BEAST<sup>29</sup> v1.8.2 was initially run on a recombination-  
450 masked SNP-only alignment containing 284 variable sites, applying a correction for invariant  
451 sites using the constantPatterns argument, in triplicate using an Uncorrelated Relaxed Clock  
452 model, assuming constant population size, lognormal population distribution, GTR  
453 substitution model, diffuse gamma distribution prior (shape 0.001, scale 1000), with a  
454 burnin of 10 million cycles followed by 100 million MCMC cycles. All MCMC chains  
455 converged, and on inspection of the marginal distribution of ucl.d.stdev we could not reject  
456 a Strict Clock. We therefore repeated the analysis using a Strict Clock model, using the same  
457 models and priors and assuming a starting molecular clock rate of  $3.6 \times 10^{-4}$  as described by  
458 others<sup>14</sup>. We used the Marginal Likelihood Estimates from the triplicate BEAST runs as input  
459 to Path Sampling and Stepping Stone Sampling analyses<sup>67,68</sup> and determined that the Strict  
460 Constant model was optimal for this dataset. To further confirm the temporal signal in our  
461 tree, we used the TIPDATINGBEAST package<sup>69</sup> in R<sup>70</sup> to resample tip-dates from our  
462 alignment, generating 20 new datasets with randomly assigned dates – BEAST analysis using  
463 the same Strict Clock prior conditions found no evidence of temporal signal in these  
464 replicates, indicating that the signal in our tree was not found by chance (Supplementary  
465 Figure 2).

466

467 Macrolide resistant SNPs were inferred using ARIBA<sup>34</sup>, which performs localised assembly  
468 and mapping in comparison with a custom reference database containing 23S sequences  
469 from Nichols (NR\_076156.1) and SS14 reference strains (NR\_076531.1).

470

471 Processing of data, and all statistical analysis was performed in R<sup>70</sup> v3.4.1, primarily using  
472 the phytools and ape packages. Phylogenies were plotted using ggtree<sup>71</sup>, and figures were  
473 produced using ggplot2<sup>72</sup>. All code used in the downstream analysis is available in  
474 Supplementary File 3.

475

## 476 Acknowledgements

477 The authors thank the sequencing team at Wellcome Sanger Institute; S Harris for access to  
478 local scripts; A Wailan for discussions around rPinecone; D Domman for helpful advice and  
479 discussion during analysis; M Fookes for initial pilot work and bait design for SureSelect; B  
480 Molini, and C Godornes at University of Washington for provision of strains; staff at  
481 University College London Hospital and clinical and sexual health staff at the Mortimer  
482 Market Clinic, London for UK sample provision. MM was supported by a Wellcome Trust  
483 Clinical Research Fellowship (102807). Strains from the University of Washington were  
484 supported by NIH grants R01 NS34235 to CMM, and R01 AI 34616 and R01 AI 42143 to SAL.  
485 MAB and NRT are supported by Wellcome funding to the Sanger Institute.

486

## 487 Author Contributions

488 Conceived and designed the study: NRT, SAL, MAB, AVN, MM. Collected and collated  
489 samples: SAL, CMM, MM, AVN, PF. Performed the laboratory work: MAB, SKS, LCT. Analysed  
490 the data: MAB. Wrote the initial draft of the manuscript: MAB. All authors viewed and  
491 contributed to the final manuscript.

492

## 493 Competing Interests

494 The authors have no competing interests to declare.

495

## 496 References

- 497 1. Tampa, M., Sarbu, I., Matei, C., Benea, V. & Georgescu, S. Brief History of Syphilis. *J.*  
498 *Med. Life* **7**, 4–10 (2014).
- 499 2. Chesson, H. W., Dee, T. S. & Aral, S. O. AIDS mortality may have contributed to the  
500 decline in syphilis rates in the United States in the 1990s. *Sex. Transm. Dis.* **30**, 419–424  
501 (2003).
- 502 3. Fenton, K. A. *et al.* Infectious syphilis in high-income settings in the 21st century. *Lancet*  
503 *Infect. Dis.* **8**, 244–253 (2008).
- 504 4. Centers for Disease Control. Syphilis - 2016 STD Surveillance Report. (2017). Available at:  
505 <https://www.cdc.gov/std/stats16/Syphilis.htm>. (Accessed: 2nd July 2018)

- 506 5. Zhou, Y. *et al.* Prevalence of HIV and syphilis infection among men who have sex with  
507 men in China: a meta-analysis. *BioMed Res. Int.* **2014**, 620431 (2014).
- 508 6. Public Health England. Sexually transmitted infections and screening for chlamydia in  
509 England, 2017. (2018).
- 510 7. European Centre for Disease Prevention and Control. Sexually transmitted infections in  
511 Europe 2013. (2015).
- 512 8. Mohammed, H. *et al.* Increase in Sexually Transmitted Infections among Men Who Have  
513 Sex with Men, England, 2014. *Emerg. Infect. Dis.* **22**, 88–91 (2016).
- 514 9. Edmondson, D. G., Hu, B. & Norris, S. J. Long-Term In Vitro Culture of the Syphilis  
515 Spirochete *Treponema pallidum* subsp. *pallidum*. *mBio* **9**, e01153-18 (2018).
- 516 10. Lafond, R. E. & Lukehart, S. A. Biological basis for syphilis. *Clin. Microbiol. Rev.* **19**, 29–49  
517 (2006).
- 518 11. Christiansen, M. T. *et al.* Whole-genome enrichment and sequencing of Chlamydia  
519 trachomatis directly from clinical samples. *BMC Infect. Dis.* **14**, 591 (2014).
- 520 12. Depledge, D. P. *et al.* Specific Capture and Whole-Genome Sequencing of Viruses from  
521 Clinical Samples. *PLoS ONE* **6**, e27805 (2011).
- 522 13. Pinto, M. *et al.* Genome-scale analysis of the non-cultivable *Treponema pallidum* reveals  
523 extensive within-patient genetic variation. *Nat. Microbiol.* **2**, 16190 (2016).
- 524 14. Arora, N. *et al.* Origin of modern syphilis and emergence of a pandemic *Treponema*  
525 *pallidum* cluster. *Nat. Microbiol.* **2**, 16245 (2016).

- 526 15. Marks, M. *et al.* Diagnostics for yaws eradication: insights from direct next generation  
527 sequencing of cutaneous strains of *Treponema pallidum*. *Clin. Infect. Dis.* (2017).  
528 doi:10.1093/cid/cix892
- 529 16. Nechvátal, L. *et al.* Syphilis-causing strains belong to separate SS14-like or Nichols-like  
530 groups as defined by multilocus analysis of 19 *Treponema pallidum* strains. *Int. J. Med.*  
531 *Microbiol.* **304**, 645–653 (2014).
- 532 17. Lukehart, S. A. *et al.* Macrolide resistance in *Treponema pallidum* in the United States  
533 and Ireland. *N. Engl. J. Med.* **351**, 154–158 (2004).
- 534 18. Šmajš, D., Paštěková, L. & Grillová, L. Macrolide Resistance in the Syphilis Spirochete,  
535 *Treponema pallidum* ssp. *pallidum*: Can We Also Expect Macrolide-Resistant Yaws  
536 Strains? *Am. J. Trop. Med. Hyg.* **93**, 678–683 (2015).
- 537 19. WHO. Eradication of yaws – the Morges Strategy. *Wkly Epidemiol Rec* **87**, 189–194  
538 (2012).
- 539 20. Mitjà, O. *et al.* Re-emergence of yaws after single mass azithromycin treatment followed  
540 by targeted treatment: a longitudinal study. *The Lancet* **391**, 1599–1607 (2018).
- 541 21. Giacani, L. *et al.* Complete Genome Sequence and Annotation of the *Treponema*  
542 *pallidum* subsp. *pallidum* Chicago Strain. *J. Bacteriol.* **192**, 2645–2646 (2010).
- 543 22. Giacani, L. *et al.* Complete Genome Sequence of the *Treponema pallidum* subsp.  
544 *pallidum* Sea81-4 Strain. *Genome Announc.* **2**, (2014).
- 545 23. Sun, J. *et al.* Tracing the origin of *Treponema pallidum* in China using next-generation  
546 sequencing. *Oncotarget* **7**, 42904–42918 (2016).

- 547 24. Matějková, P. *et al.* Complete genome sequence of *Treponema pallidum* ssp. *pallidum*  
548 strain SS14 determined with oligonucleotide arrays. *BMC Microbiol.* **8**, 76 (2008).
- 549 25. Pětrošová, H. *et al.* Resequencing of *Treponema pallidum* ssp. *pallidum* Strains Nichols  
550 and SS14: Correction of Sequencing Errors Resulted in Increased Separation of Syphilis  
551 *Treponeme* Subclusters. *PLOS ONE* **8**, e74319 (2013).
- 552 26. Tong, M.-L. *et al.* Whole genome sequence of the *Treponema pallidum* subsp. *pallidum*  
553 strain Amoy: An Asian isolate highly similar to SS14. *PLoS ONE* **12**, (2017).
- 554 27. Čejková, D. *et al.* Whole Genome Sequences of Three *Treponema pallidum* ssp.  
555 *pertenue* Strains: Yaws and Syphilis *Treponemes* Differ in Less than 0.2% of the Genome  
556 Sequence. *PLoS Negl. Trop. Dis.* **6**, e1471 (2012).
- 557 28. Pětrošová, H. *et al.* Whole Genome Sequence of *Treponema pallidum* ssp. *pallidum*,  
558 Strain Mexico A, Suggests Recombination between Yaws and Syphilis Strains. *PLoS Negl.*  
559 *Trop. Dis.* **6**, e1832 (2012).
- 560 29. Suchard, M. A. *et al.* Bayesian phylogenetic and phylodynamic data integration using  
561 BEAST 1.10. *Virus Evol.* **4**, (2018).
- 562 30. Wailan, A. M. *et al.* rPinecone: Define sub-lineages of a clonal expansion via a  
563 phylogenetic tree. *bioRxiv* 404624 (2018). doi:10.1101/404624
- 564 31. Stamm, L. V. & Bergen, H. L. A Point Mutation Associated with Bacterial Macrolide  
565 Resistance Is Present in Both 23S rRNA Genes of an Erythromycin-Resistant *Treponema*  
566 *pallidum* Clinical Isolate. *Antimicrob. Agents Chemother.* **44**, 806–807 (2000).

- 567 32. Matějková, P. *et al.* Macrolide treatment failure in a case of secondary syphilis: a novel  
568 A2059G mutation in the 23S rRNA gene of *Treponema pallidum* subsp. *pallidum*. *J. Med.*  
569 *Microbiol.* **58**, 832–836 (2009).
- 570 33. Molini, B. J. *et al.* Macrolide Resistance in *Treponema pallidum* Correlates With 23S  
571 rDNA Mutations in Recently Isolated Clinical Strains. *Sex. Transm. Dis.* **43**, 579–583  
572 (2016).
- 573 34. Hunt, M. *et al.* ARIBA: rapid antimicrobial resistance genotyping directly from  
574 sequencing reads. *Microb. Genomics* **3**, (2017).
- 575 35. Weill, F.-X. *et al.* Genomic history of the seventh pandemic of cholera in Africa. *Science*  
576 **358**, 785–789 (2017).
- 577 36. Hadfield, J. *et al.* Comprehensive global genome dynamics of *Chlamydia trachomatis*  
578 show ancient diversification followed by contemporary mixing and recent lineage  
579 expansion. *Genome Res.* **27**, 1220–1229 (2017).
- 580 37. Strouhal, M. *et al.* Complete genome sequences of two strains of *Treponema pallidum*  
581 subsp. *pertenue* from Ghana, Africa: Identical genome sequences in samples isolated  
582 more than 7 years apart. *PLoS Negl. Trop. Dis.* **11**, e0005894 (2017).
- 583 38. Grimes, M. *et al.* Two Mutations associated with Macrolide Resistance in *Treponema*  
584 *pallidum*: Increasing Prevalence and Correlation with Molecular Strain Type in Seattle,  
585 Washington. *Sex. Transm. Dis.* **39**, 954–958 (2012).
- 586 39. WHO. WHO guidelines for the treatment of *Treponema pallidum* (syphilis). (2016).
- 587 40. Centers for Disease Control. Sexually Transmitted Diseases Treatment Guidelines, 2015.  
588 *Morb. Mortal. Wkly. Rep.* **64**, (2015).



- 589 41. Marra, C. M. *et al.* Antibiotic Selection May Contribute to Increases in Macrolide-  
590 Resistant *Treponema pallidum*. *J. Infect. Dis.* **194**, 1771–1773 (2006).
- 591 42. Hicks, L. A., Taylor, T. H. & Hunkler, R. J. U.S. Outpatient Antibiotic Prescribing, 2010. *N.*  
592 *Engl. J. Med.* **368**, 1461–1462 (2013).
- 593 43. Kong, F. Y. S. *et al.* Pharmacokinetics of a single 1g dose of azithromycin in rectal tissue  
594 in men. *PLOS ONE* **12**, e0174372 (2017).
- 595 44. Nurse-Findlay, S. *et al.* Shortages of benzathine penicillin for prevention of mother-to-  
596 child transmission of syphilis: An evaluation from multi-country surveys and stakeholder  
597 interviews. *PLOS Med.* **14**, e1002473 (2017).
- 598 45. Chen, X.-S. *et al.* High prevalence of azithromycin resistance to *Treponema pallidum* in  
599 geographically different areas in China. *Clin. Microbiol. Infect.* **19**, 975–979 (2013).
- 600 46. Lu, H. *et al.* High frequency of the 23S rRNA A2058G mutation of *Treponema pallidum* in  
601 Shanghai is associated with a current strategy for the treatment of syphilis. *Emerg.*  
602 *Microbes Infect.* **4**, e10 (2015).
- 603 47. Taylor, M. *et al.* Revisiting strategies to eliminate mother-to-child transmission of  
604 syphilis. *Lancet Glob. Health* **6**, e26–e28 (2018).
- 605 48. Baker, S., Thomson, N., Weill, F.-X. & Holt, K. E. Genomic insights into the emergence  
606 and spread of antimicrobial-resistant bacterial pathogens. *Science* **360**, 733–738 (2018).
- 607 49. WHO. Global action plan on antimicrobial resistance. (2015).
- 608 50. Lukehart, S. A. & Marra, C. M. Isolation and laboratory maintenance of *Treponema*  
609 *pallidum*. *Curr. Protoc. Microbiol.* **Chapter 12**, Unit 12A.1 (2007).

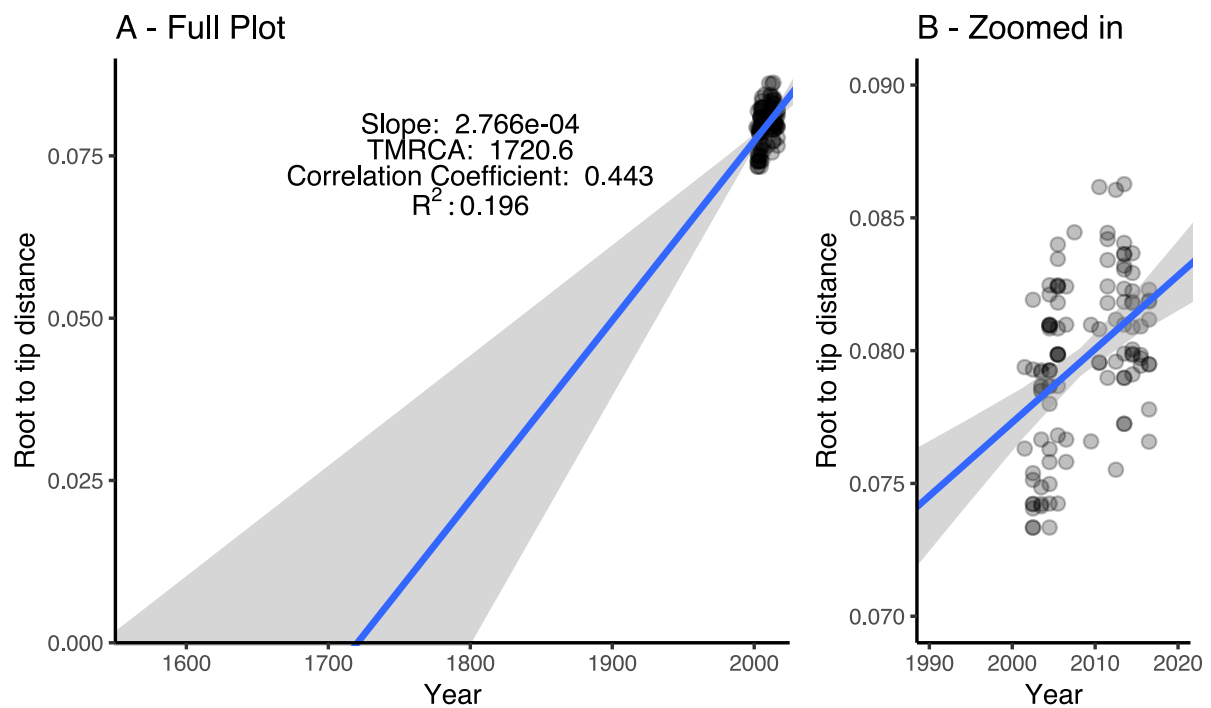
- 610 51. Wood, D. E. & Salzberg, S. L. Kraken: ultrafast metagenomic sequence classification  
611 using exact alignments. *Genome Biol.* **15**, R46 (2014).
- 612 52. Bolger, A. M., Lohse, M. & Usadel, B. Trimmomatic: a flexible trimmer for Illumina  
613 sequence data. *Bioinformatics* **30**, 2114–2120 (2014).
- 614 53. Quinlan, A. R. & Hall, I. M. BEDTools: a flexible suite of utilities for comparing genomic  
615 features. *Bioinformatics* **26**, 841–842 (2010).
- 616 54. Li, H. Aligning sequence reads, clone sequences and assembly contigs with BWA-MEM.  
617 *arXiv* (2013). doi:1303.3997v1 [q-bio.GN]
- 618 55. Van der Auwera, G. A. *et al.* From FastQ data to high confidence variant calls: the  
619 Genome Analysis Toolkit best practices pipeline. *Curr. Protoc. Bioinforma. Ed. Board*  
620 *Andreas Baxevanis Al* **11**, 11.10.1-11.10.33 (2013).
- 621 56. Li, H. *et al.* The Sequence Alignment/Map format and SAMtools. *Bioinformatics* **25**,  
622 2078–2079 (2009).
- 623 57. Croucher, N. J. *et al.* Rapid phylogenetic analysis of large samples of recombinant  
624 bacterial whole genome sequences using Gubbins. *Nucleic Acids Res.* gku1196 (2014).  
625 doi:10.1093/nar/gku1196
- 626 58. Nguyen, L.-T., Schmidt, H. A., von Haeseler, A. & Minh, B. Q. IQ-TREE: A Fast and  
627 Effective Stochastic Algorithm for Estimating Maximum-Likelihood Phylogenies. *Mol.*  
628 *Biol. Evol.* **32**, 268–274 (2015).
- 629 59. Lewis, P. O. A Likelihood Approach to Estimating Phylogeny from Discrete Morphological  
630 Character Data. *Syst. Biol.* **50**, 913–925 (2001).

- 631 60. Kalyaanamoorthy, S., Minh, B. Q., Wong, T. K. F., Haeseler, A. von & Jermini, L. S.  
632 ModelFinder: fast model selection for accurate phylogenetic estimates. *Nat. Methods*  
633 **14**, 587–589 (2017).
- 634 61. Kimura, M. Estimation of evolutionary distances between homologous nucleotide  
635 sequences. *Proc. Natl. Acad. Sci.* **78**, 454–458 (1981).
- 636 62. Soubrier, J. *et al.* The Influence of Rate Heterogeneity among Sites on the Time  
637 Dependence of Molecular Rates. *Mol. Biol. Evol.* **29**, 3345–3358 (2012).
- 638 63. Hoang, D. T., Chernomor, O., Haeseler, A. von, Minh, B. Q. & Le, V. S. UFBoot2:  
639 Improving the Ultrafast Bootstrap Approximation. *bioRxiv* 153916 (2017).  
640 doi:10.1101/153916
- 641 64. Minh, B. Q., Nguyen, M. A. T. & von Haeseler, A. Ultrafast Approximation for  
642 Phylogenetic Bootstrap. *Mol. Biol. Evol.* **30**, 1188–1195 (2013).
- 643 65. Pupko, T., Pe, I., Shamir, R. & Graur, D. A Fast Algorithm for Joint Reconstruction of  
644 Ancestral Amino Acid Sequences. *Mol. Biol. Evol.* **17**, 890–896 (2000).
- 645 66. Rambaut, A., Lam, T. T., Max Carvalho, L. & Pybus, O. G. Exploring the temporal  
646 structure of heterochronous sequences using TempEst (formerly Path-O-Gen). *Virus*  
647 *Evol.* **2**, (2016).
- 648 67. Baele, G. & Lemey, P. Bayesian evolutionary model testing in the phylogenomics era:  
649 matching model complexity with computational efficiency. *Bioinformatics* **29**, 1970–  
650 1979 (2013).

- 651 68. Baele, G. *et al.* Improving the accuracy of demographic and molecular clock model  
652 comparison while accommodating phylogenetic uncertainty. *Mol. Biol. Evol.* **29**, 2157–  
653 2167 (2012).
- 654 69. Rieux, A. & Khatchikian, C. E. tipdatingbeast: an r package to assist the implementation  
655 of phylogenetic tip-dating tests using beast. *Mol. Ecol. Resour.* **17**, 608–613
- 656 70. R Core Team. *R: A Language and Environment for Statistical Computing*. (R Foundation  
657 for Statistical Computing, 2014).
- 658 71. Yu, G., Smith, D., Zhu, H., Guan, Y. & Lam, T. T.-Y. *ggtree: an R package for visualization*  
659 *and annotation of phylogenetic tree with different types of meta-data*.
- 660 72. Wickham, H. *ggplot2: Elegant Graphics for Data Analysis*. (Springer-Verlag, 2009).
- 661

## 662 Supplementary Figures

663 Supplementary Figure 1. Root-to-tip regression analysis of tip dates against branch lengths  
664 showing a correlation of 0.443 and R<sup>2</sup> of 0.196, providing evidence for temporal signal in  
665 the Maximum Likelihood tree, performed in TempEst using clinically derived genomes from  
666 both Nichols and SS14 lineages. Plots show tip points and linear regression (with standard  
667 error) for full timeline (A) and zoomed in to only include sampled tipdates (B). Each data  
668 point is coloured grey, with darker shading indicating multiple overlapping points.



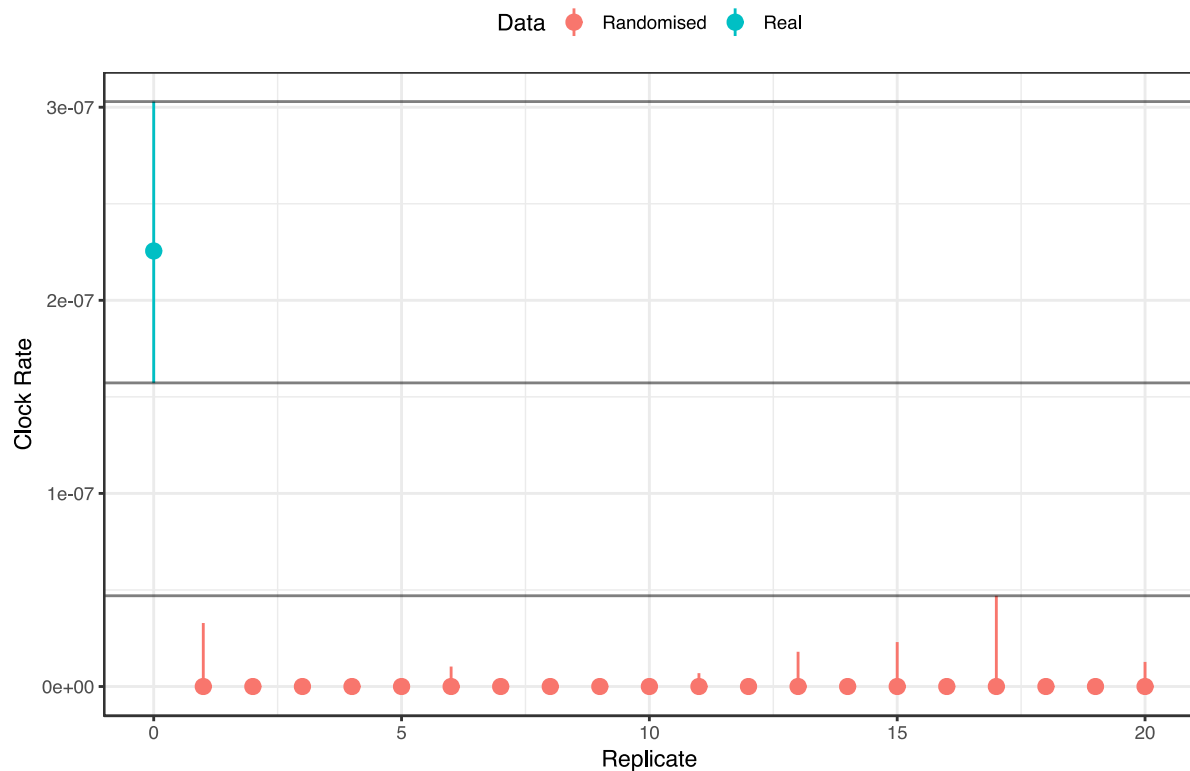
669

670

671

672 Supplementary Figure 2. Tip date resampling analysis performed using twenty datasets with  
673 randomised tip dates generated from the original Strict Clock analysis and run in BEAST  
674 under the same conditions. Median clock rate for the real tree was  $2.26 \times 10^{-7}$ , whilst all

675 randomly assigned datasets gave substantially lower clock rates, with the highest median  
676 clock rate obtained at  $1.90 \times 10^{-12}$ . This indicates that the temporal signal observed in our  
677 tree was not obtained by chance, and provides further evidence for a temporal signal in the  
678 multiple sequence alignment.



679

680

681

682 Supplementary Table 1. Full sample metadata (Excel Sheet) for this study, including  
683 sequence naming used in this paper, in other publications, and on GenBank, ENA Accessions  
684 for all new genomes, as well as results of lineage and sub-lineage typing and inference of  
685 genotypic macrolide resistance.

686

687 Supplementary Table 2. List of genomic regions behaving in a non-clocklike manner and  
688 masked due to hypervariable, recombining or repetitive elements.

689

690 Supplementary File 3. Rnotebook (HTML format) containing all downstream code used to  
691 generate primary figures and statistics.